CLINICAL RESEARCH ARTICLE

Heart rate variability spectrum characteristics in children with sleep apnea

Adrián Martín-Montero [1], Gonzalo C. Gutiérrez-Tobal[1,2], Leila Kheirandish-Gozal[3], Jorge Jiménez-García[1], Daniel Álvarez[1,2,4], Félix del Campo[1,2,4], David Gozal[3] and Roberto Hornero[1,2]

BACKGROUND: Classic spectral analysis of heart rate variability (HRV) in pediatric sleep apnea–hypopnea syndrome (SAHS) traditionally evaluates the very low frequency (VLF: 0–0.04 Hz), low frequency (LF: 0.04–0.15 Hz), and high frequency (HF: 0.15–0.40 Hz) bands. However, specific SAHS-related frequency bands have not been explored.
METHODS: One thousand seven hundred and thirty-eight HRV overnight recordings from two pediatric databases (0–13 years) were evaluated. The first one (981 children) served as training set to define new HRV pediatric SAHS-related frequency bands. The associated relative power (RP) were computed in the test set, the Childhood Adenotonsillectomy Trial database (CHAT, 757 children). Their relationships with polysomnographic variables and diagnostic ability were assessed.
RESULTS: Two new specific spectral bands of pediatric SAHS within 0–0.15 Hz were related to duration of apneic events, number of awakenings, and wakefulness after sleep onset (WASO), while an adaptive individual-specific new band from HF was related to oxyhemoglobin desaturations, arousals, and WASO. Furthermore, these new spectral bands showed improved diagnostic ability than classic HRV.
CONCLUSIONS: Novel spectral bands provide improved characterization of pediatric SAHS. These findings may pioneer a better understanding of the effects of SAHS on cardiac function and potentially serve as detection biomarkers.

Pediatric Research _####################_; https://doi.org/10.1038/s41390-020-01138-2

IMPACT:

- New specific heart rate variability (HRV) spectral bands are identified and characterized as potential biomarkers in pediatric sleep apnea.
- Spectral band BW1 (0.001–0.005 Hz) is related to macro sleep disruptions.
- Spectral band BW2 (0.028–0.074 Hz) is related to the duration of apneic events.
- An adaptive spectral band within the respiratory range, termed ABW3, is related to oxygen desaturations.
- The individual and collective diagnostic ability of these novel spectral bands outperforms classic HRV bands.

INTRODUCTION

Pediatric sleep apnea–hypopnea syndrome (SAHS) is a respiratory disturbance defined by periods of total airflow interruption (apnea) and/or significant airflow decrease (hypopnea).[1,2] It is highly prevalent, with up to 5% of the general pediatric population being affected,[2] and has been related to increased risk for several cardiovascular morbidities, such as left and right ventricular hypertrophy, increases in systemic and pulmonary vascular blood pressure, alterations in autonomic regulation, and cerebral blood flow and perfusion.[2]

Pediatric SAHS is traditionally diagnosed using overnight polysomnography (PSG).[3,4] To this effect, children will spend a night in a laboratory, while up to 32 biomedical signals are registered, including the electrocardiogram (ECG).[4] These signals are then evaluated and scored by medical experts using well-defined criteria, and several indices of respiratory disturbance are extracted, among which the apnea–hypopnea index (AHI) is the most frequently used. AHI consists of the total of apneic and hypopneic events per hour of sleep (e/h) and defines both SAHS presence and severity.[4] Although the PSG is accepted as the reference diagnostic method for SAHS, it is time-consuming, expensive, and potentially distressing for pediatric subjects.[5,6] In the search for alternatives that can address these issues while also evaluating cardiovascular morbidity risks, various studies have focused on the analysis of an abbreviated set of the signals containing cardiac information to gain insights into the cardiac dynamics in children with SAHS.[5,6]

Heart rate variability (HRV), a signal derived from the ECG, is a measure of the fluctuation over time of the period between successive heartbeats.[7] HRV assesses cardiac health and provides a better understanding of autonomic nervous system (ANS) homeostasis, which regulates cardiac activity.[7] The ANS controls

2

the response of the heart to respiratory events, with a recurrent pattern of progressive bradycardia/abrupt tachycardia reflecting activation and deactivation of two of the ANS branches, namely, the parasympathetic and the sympathetic nervous systems.[8,9] This periodic behavior has motivated previous spectral analyses of HRV, both in adults[10–13] and children.[14–25]

Past studies analyzed the classical HRV spectral bands: very low frequency (VLF), low frequency (LF), and high frequency (HF) bands, which have fixed boundaries (0–0.04, 0.04–0.15, and 0.15–0.40 Hz, respectively).[26] Nevertheless, some recent work in adults indicates that SAHS modifies the HRV spectrum in a frequency range comprising portions of the VLF and LF bands,[10] suggesting that specific SAHS-related frequency bands may also be present in children with SAHS. Furthermore, previous studies have reported that HF, which is known as a respiratory-modulated band,[7] is strongly influenced by age, regardless of health condition.[27] Likewise, it has been shown that cardio-respiratory coordination increases during apneic events,[28] which underlines the influence of the respiration on heart rate. Age-related alterations are reflected in the frequency at which respiratory peak within HF occurs,[29–32] suggesting that a subject-adaptive analysis is more accurate for this frequency range. Notwithstanding, all previous HRV analyses in pediatric SAHS neglected to incorporate the changes in respiration related to age.[33]

Based on these considerations, we hypothesized that pediatric SAHS-specific frequency bands of interest are present and embedded in the ECG, and consequently, our main objective was to evaluate and characterize the HRV spectrum in a broad population of children with SAHS. To this effect, we delineated two specific objectives for this study: (i) identification of putative novel frequency bands, taking into account SAHS severity groups and subject-specific considerations, and (ii) comparison of their diagnostic ability against the classic HRV spectral bands.

METHODS

Subjects and signals under study
This work involved 1738 pediatric subjects aged between 0 and 13 years. Two large cohorts were included: a database from the University of Chicago (UofC),[34,35] which includes 981 children referred to the Pediatric Sleep Unit at Comer Children's Hospital of the UofC (Chicago, IL, USA) suspected of suffering from SAHS; and a second cohort composed of 757 children from the dataset of the multicenter Childhood Adenotonsillectomy Trial (CHAT) database.[36,37] UofC database was established as the training set, while the CHAT database served as the test set.

The informed consent of all children caretakers from the UofC sample were obtained, and the Ethics Committee of the Comer Children's Hospital of the University of Chicago approved the protocol (#11-0268-AM017, #09-115-B-AM031, and #IRB14–1241). Diagnosis was reached using a digital PSG system (Polysmith, Nihon Kohden America INC., Irvine, CA, USA). ECG was recorded at sample frequencies of 200 or 500 Hz.

For the CHAT sample, details corresponding to entire protocol are available in the supplementary material of ref.[37] Specifically, a total of 779 nocturnal PSGs of children aged between 5 and 10 years were included. ECG signals were acquired at sampling frequencies of 50, 200, 250, 256, or 512 Hz. Finally, 757 subjects were used from this dataset since 22 were excluded after applying the signal pre-processing protocol explained below.

All the subjects included in this study were diagnosed by pediatric sleep specialists from the different centers, and their sleep studies were scored in accordance with the American Academy of Sleep Medicine (AASM) rules.[38] The AHI was extracted from the nocturnal PSGs and used to establish SAHS severity. Based on previous studies,[35,39–42] three typical AHI thresholds were selected (1, 5, and 10 e/h) for the division into four severity groups: the groups no-SAHS (AHI < 1 e/h), mild SAHS (1 ≤ AHI < 5 e/h),

Table 1. Clinical and demographic data from children included in the study.

	All	Training group (UofC)	Test group (CHAT)
Subjects (n)	1738	981	757
Age (years)	6.4 [3.3]	6.0 [6.0]	7.0 [2.4]
Males (n)	962 (55.35%)	602 (61.37%)	360 (47.95%)
BMI (kg/m²)	17.63 [5.37]	18.02 [5.86]	17.28 [4.64]
AHI (e/h)	2.23 [5.27]	3.8 [7.76]	1.46 [2.07]
AHI ≥ 1 (e/h)	1309 (75.31%)	808 (82.36%)	501 (66.18%)
AHI ≥ 5 (e/h)	519 (29.86%)	407 (41.49%)	112 (14.80%)
AHI ≥ 10 (e/h)	298 (17.15%)	229 (23.34%)	69 (9.11%)

Data are shown as median [interquartile range] or n (percentage).
UofC University of Chicago, *CHAT* Childhood Adenotonsillectomy Trial, *BMI* Body Mass Index, *AHI* apnea–hypopnea index.

moderate SAHS (5 ≤ AHI < 10 e/h), and severe SAHS (AHI ≥ 10 e/h). Table 1 shows the clinical and demographic data of the population considered.

The ECG signals from both databases were equally pre-processed. First, the 15 initial and final minutes from every signal were removed to avoid early and late artifact periods. Then all recordings lasting <3 h were excluded. Afterwards, the HRV was extracted following an algorithm based on the Hilbert transform proposed by Benítez et al.[43] The first stage of this algorithm consists in computing the first-order derivative after baseline correction of the ECG.[43] The Hilbert transform is subsequently computed for this derivative to locate regions of high probability of containing R peaks around true R peaks. Later, a search for actual R peak positions is conducted by establishing a threshold derived from the root mean square of the Hilbert transform for each region.[43] Once the R peaks are detected, the R–R intervals conforming HRV signals are easily calculated.[7] Those beats that did not meet the following criteria were considered as physiologically impossible and removed:[11] (i) 0.33 s < R–R interval < 1.5 s and (ii) difference to the previous R–R interval >0.66 s.
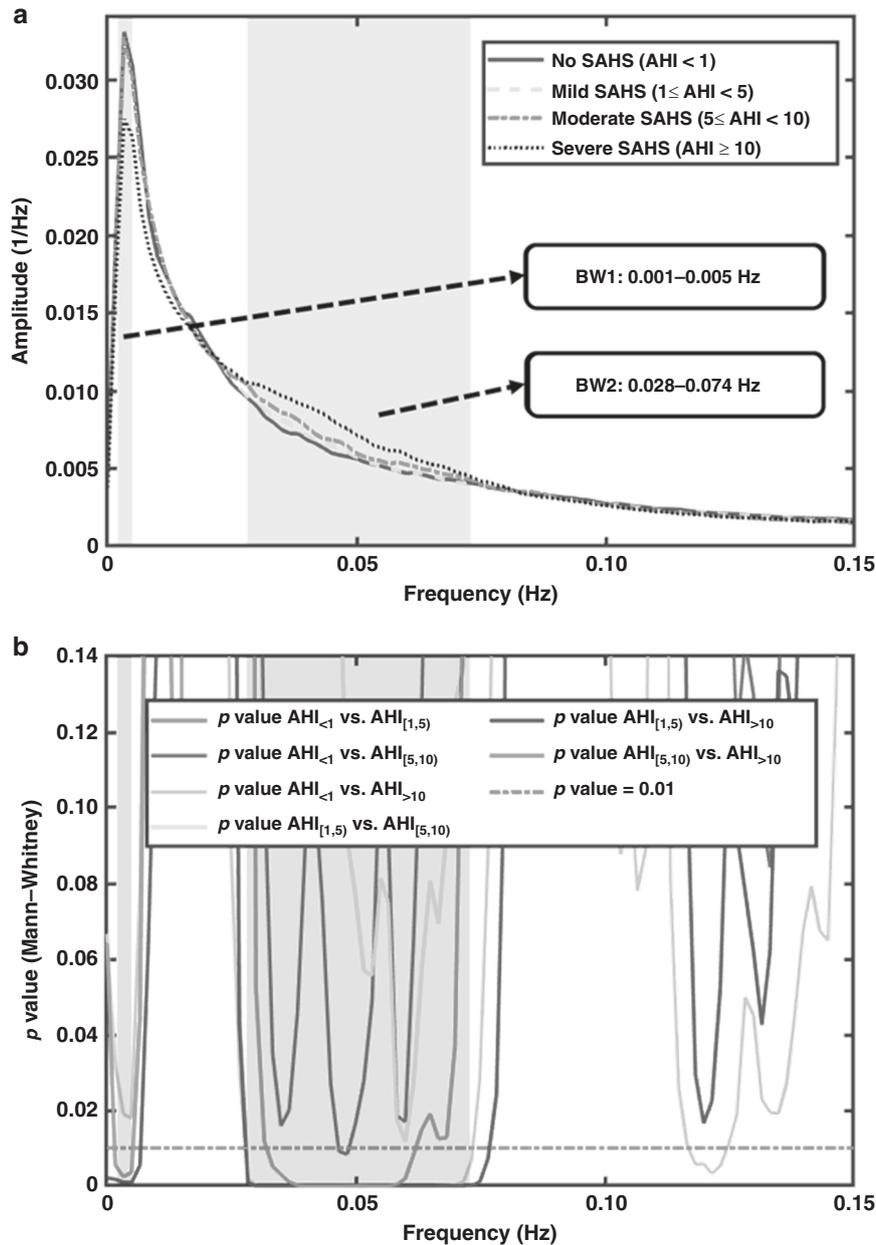
Finally, the HRV signals were resampled to a constant rate in order to obtain equally spaced time samples and allow their analysis in the frequency domain. This rate of 3.41 Hz[10,11] was chosen to evaluate 5-min epochs as a trade-off between using a power of two window-length (2^{10} samples) with fast Fourier transform (FFT) and not adding unnecessary estimated data. Five-min epochs were chosen as it is the maximum length where stationarity can be assumed, in order to compute spectral analysis.[11]

Determination of spectral bands of interest
Welch's periodogram was applied to estimate the power spectral density (PSD) of the HRV.[44] A Hamming Window of 2^{10} (50% overlap) and a FFT of 2^{11} points were used. Then a normalization was applied to PSDs (PSDn) by dividing the amplitude values at each frequency by the corresponding total spectral power. This normalization is intended to minimize the differences due to individual conditions other than SAHS.[45] The bands of interest were defined based on the PSDns from the training group.

Due to the considerations mentioned in the first section, we defined the spectral bands of interest by combining two different analyses depending on the frequency range: in 0–0.15 Hz, which should not be influenced by age, and in 0.15–0.4 Hz, where an adaptive analysis was adopted.

The adaptive analysis in the HF range was based on previous studies of Milagro et al.[31,32] Similar to those studies, we chose a
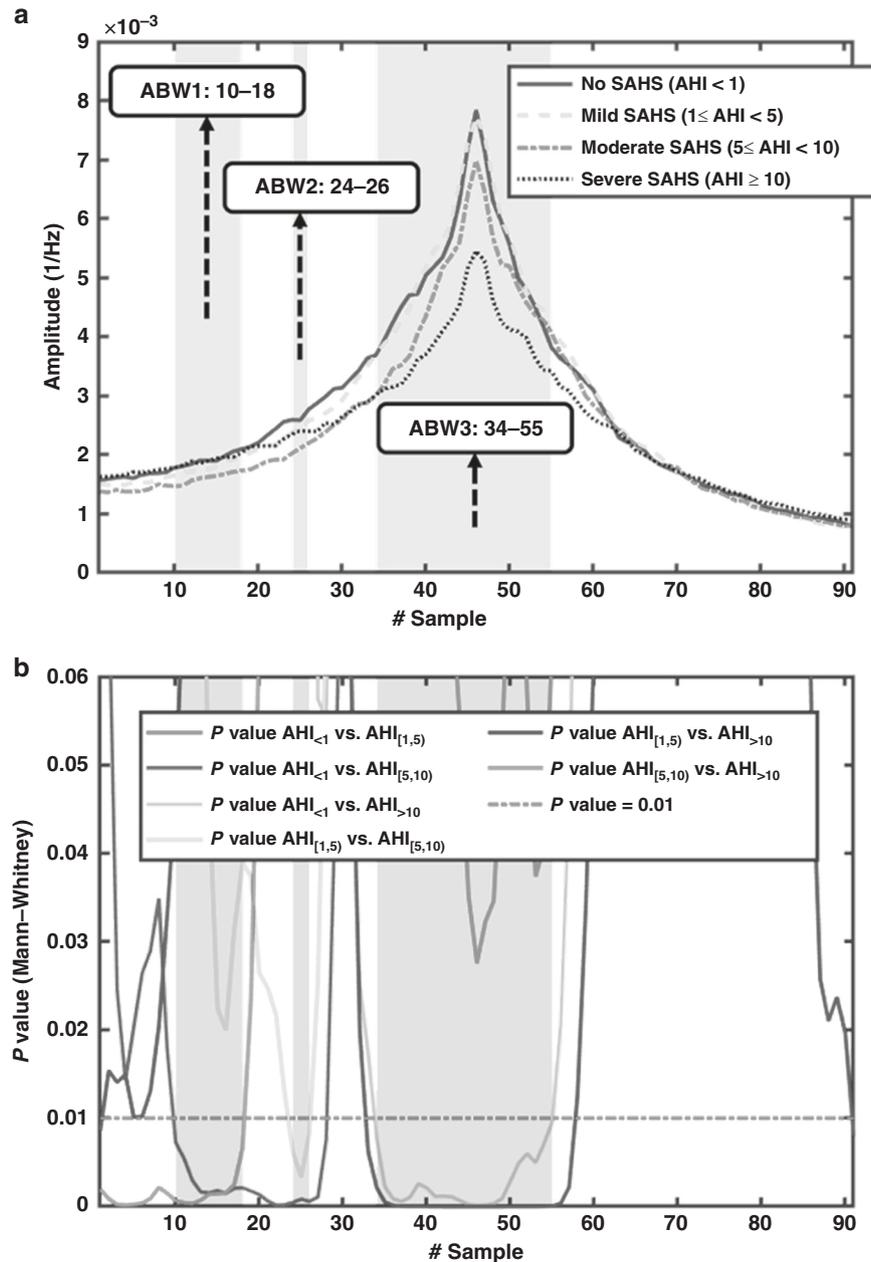
Heart rate variability spectrum characteristics in children with sleep...
A Martín-Montero et al.

3

Fig. 1 PSDns analysis in the range 0-0.15 Hz. a Averaged PSDns in the 0–0.15 Hz band in the training set for the four severity groups. **b** p value for each frequency in each comparison between SAHS severity groups after Bonferroni correction in the training group for the range 0–0.15 Hz. Gray-shaded areas represent those ranges where statistical differences were found.

0.15-Hz adaptive range centered in the individual respiratory peak frequency. However, rather than obtaining this central frequency from the impedance pneumography signal, we approximated the individual peak position as the frequency where the highest PSD value is found in the HF range. As it was previously reported, this approximation is an accurate estimation of the respiratory peak.[30] Thereby, we obtained an adaptive bandwidth of 0.15 Hz for each subject, formed by 91 samples extracted from the PSD of HF.

Once we defined the adaptive band for each individual, the selection of bands of interest in both the range 0–0.15 Hz and the adaptive range was based on statistical differences between PSDns from the training set severity groups. We computed the non-parametric Mann–Whitney U test for each two severity groups comparing frequency by frequency (in the band of 0–0.15 Hz) or sample by sample (in the adaptive one) the

amplitude values from the PSDns. Therefore, six statistical tests were computed. After applying the Bonferroni correction, we selected p value < 0.01 as the significance level and established as bands of interest those ranges where at least two of the tests yielded statistical differences.

Figures 1a and 2a show the averaged PSDns of the four SAHS groups in the 0–0.15 Hz and the adaptive band, respectively. Some differences between groups can be appreciated, with shaded areas as the ranges where statistical differences were found. Figures 1b and 2b show the p values reached. According to this methodology, the bands of interest selected in the range 0–0.15 Hz were BW1 [0.001–0.005] Hz and BW2 [0.028–0.074] Hz. Correspondingly, the adaptive bands selected in the adaptive range were ABW1 [samples 10–18], ABW2 [samples 24–26], and ABW3 [samples 34–55].

Heart rate variability spectrum characteristics in children with sleep...
A Martín-Montero et al.

4

Fig. 2 PSDns analysis in the adaptive range. a Averaged PSDns in the adaptive band in the training set for the four severity groups. **b** *p* value for each frequency in each comparison between SAHS severity groups after Bonferroni correction in the training set for the adaptive band selected. Gray-shaded areas represent those ranges where statistical differences were found.

Feature extraction: relative power (RP)

The sum of PSDn values in a given frequency range is known as RP. In HRV signals, spectral powers from VLF, LF, and HF bands have been commonly assessed.[7,26] LF band has been related to both sympathetic and parasympathetic tone.[7] The HF band is strongly related to the respiratory rhythm, as well as with the parasympathetic tone.[7,31,32] Physiological interpretation of VLF band is unclear, and it has been associated with sympathetic tone and thermoregulatory effects in long-term recordings.[7,26] The LF/HF ratio is another common explored measure and used as a reflection of the balance between sympathetic and parasympathetic tones.[7,26] Because these parameters have been widely assessed in the pediatric SAHS context,[14–25] we have chosen RP as the approach to characterize the activity in all the frequency bands considered in this study. Thus we have

computed RP of the three classical frequency bands (RP_{VLF}, RP_{LF}, RP_{HF}), the five bands of interest (RP_{BW1}, RP_{BW2}, RP_{ABW1}, RP_{ABW2}, RP_{ABW3}), and the LF/HF ratio.

Assessment of the diagnostic ability of the HRV spectrum

In order to compare the diagnostic ability of the new frequency bands of interest with the classical ones, we first evaluated the individual diagnostic performance of each parameter extracted from the HRV spectrum. This was achieved by using optimum cut-off points from the receiver operating characteristic (ROC) curve in the training set. Then thresholds of 1, 5, and 10 e/h were selected, and binary classification was performed.

The joint diagnostic performance of the parameters was evaluated by constructing two models. On the one hand, a model containing the RPs from the five bands of interest was considered.

Heart rate variability spectrum characteristics in children with sleep...
A Martín-Montero et al.

5

On the other hand, a model with the three classic RPs and the LF/HF ratio was assessed. Then two classifiers based on linear discriminant analysis (LDA) were trained in each binary classification for the three severity thresholds used in this study, and the diagnostic performance in the test set was obtained. The LDA classifier was selected due to its simplicity and its proved utility in the SAHS context.[46,47] LDA is a supervised learning algorithm that separates the input features space into decision regions, defining linear decision boundaries.[47] A discriminant score y_j (x) is computed for each class in accordance with ref. [46]:

$$y_j(x) = \mu_j^T \sum{}^{-1} x - \frac{1}{2} \mu_j^T \sum{}^{-1} \mu_j + \ln P(C_j), \quad (1)$$

where Σ is the covariance matrix and μ_j is the mean vector for class C_j and $P(C_j)$ its corresponding prior probability, i.e., the proportion of input feature vectors (x_i) belonging to class C_j. After computing each discriminant score, the class with the higher y_j is assigned to the input vector.

Statistical analysis
Features considered in this study did not fit either normality or homoscedasticity tests. For this reason, the non-parametric Kruskal–Wallis test was applied to assess statistically significant differences (p value <0.01 after Bonferroni correction) between RPs from the SAHS severity groups in both datasets. The joint and individual diagnostic performances were evaluated in terms of sensitivity (Se, proportion of subjects with SAHS correctly diagnosed), specificity (Sp, proportion of subjects without SAHS correctly diagnosed), and accuracy (Acc, proportion of subjects correctly diagnosed). We also evaluated the area under ROC curve (AUC). All these diagnostic evaluations were obtained in the test set.

Furthermore, we conducted a correlation analysis to investigate possible relationships between RPs and several polysomnographic indices related to SAHS, sleep quality, and structure. Indices related to SAHS were total AHI, obstructive AHI (OAHI), obstructive apnea index (OAI), and oxygen desaturation index (ODI). On the other hand, indices related to sleep quality and structure were the wake after sleep onset (WASO); the number of awakenings during total sleep time (#Awakenings); percentage of total sleep time spent in N1 (%N1), N2 (%N2), N3 (%N3), and REM (%REM) stages; and total arousal index (TAI, arousals per hour of sleep). Spearman's partial correlation coefficient (ρ_S) was applied to control for the influence of age in the relationships between RPs and these polysomnographic indices. In order to validate the usefulness of our new bands established on the training set, correlations were evaluated in the test set.

RESULTS
Relative powers
Table 2 shows the RPs extracted in each frequency band for each severity group (median [interquartile range]), together with the p values obtained using the Kruskal–Wallis test in both the training and the test set. RP_{BW2}, RP_{LF}, and LF/HF showed clear increases at higher SAHS severities, with RP_{BW2} and RP_{LF} showing p values <10^{-4} after Bonferroni correction (denoted as p value $\ll$ 0.01) in both sets. RP_{BW1} showed a decrease with SAHS in the two sets, as did RP_{ABW2}, RP_{ABW3}, and RP_{HF} but only in the training set for these three measures. VLF was the only band that did not show statistically significant differences in any of the two sets evaluated.

Correlation analysis in the test set
Correlation results are shown in Table 3. Spearman's partial correlation coefficient (ρ_S) is represented for each RP and variable, along with the corresponding p value. No statistically significant correlations in RP_{ABW1} and RP_{ABW2} were obtained with any of the

Table 2. Relative power values (median [interquartile range]) in the training and test sets for the four severity groups.

Feature	No SAHS	Mild SAHS	Moderate SAHS	Severe SAHS	p value
Training set					
RP_{VLF}	0.370 [0.174]	0.359 [0.163]	0.381 [0.179]	0.371 [0.164]	0.675
RP_{LF}	0.225 [0.060]	0.224 [0.075]	0.235 [0.081]	0.244 [0.090]	**≪0.01**
RP_{HF}	0.317 [0.179]	0.340 [0.195]	0.300 [0.218]	0.275 [0.213]	**<0.01**
LF/HF	0.706 [0.510]	0.697 [0.594]	0.814 [0.791]	0.892 [0.985]	**≪0.01**
RP_{BW1}	0.083 [0.055]	0.082 [0.050]	0.083 [0.047]	0.071 [0.049]	**<0.01**
RP_{BW2}	0.169 [0.054]	0.175 [0.068]	0.185 [0.086]	0.213 [0.107]	**≪0.01**
RP_{ABW1}	0.017 [0.010]	0.016 [0.009]	0.015 [0.007]	0.017 [0.010]	**<0.01**
RP_{ABW2}	0.008 [0.005]	0.007 [0.005]	0.006 [0.004]	0.005 [0.005]	**<0.01**
RP_{ABW3}	0.119 [0.110]	0.121 [0.121]	0.110 [0.115]	0.087 [0.098]	**≪0.01**
Test set					
RP_{VLF}	0.337 [0.140]	0.332 [0.155]	0.282 [0.149]	0.342 [0.186]	0.200
RP_{LF}	0.218 [0.060]	0.227 [0.063]	0.222 [0.090]	0.259 [0.110]	**≪0.01**
RP_{HF}	0.368 [0.167]	0.363 [0.184]	0.388 [0.198]	0.307 [0.217]	0.015
LF/HF	0.610 [0.407]	0.649 [0.462]	0.597 [0.539]	0.818 [0.886]	**<0.01**
RP_{BW1}	0.081 [0.044]	0.078 [0.039]	0.063 [0.045]	0.061 [0.043]	**<0.01**
RP_{BW2}	0.148 [0.055]	0.161 [0.062]	0.165 [0.078]	0.209 [0.113]	**≪0.01**
RP_{ABW1}	0.018 [0.009]	0.018 [0.009]	0.018 [0.007]	0.018 [0.010]	0.880
RP_{ABW2}	0.008 [0.005]	0.008 [0.004]	0.009 [0.005]	0.007 [0.006]	0.421
RP_{ABW3}	0.132 [0.108]	0.123 [0.107]	0.134 [0.143]	0.103 [0.093]	0.004[a]

RP Relative power, *SAHS* sleep apnea–hypopnea syndrome, *VLF* very low frequency, *LF* low frequency, *HF* high frequency.
p values < 10^{-4} after Bonferroni correction are represented as ≪0.01.
[a]Non-significant after Bonferroni correction.
p values statistically significant (<0.01 after Bonferroni correction) appears in bold.

Heart rate variability spectrum characteristics in children with sleep…
A Martín-Montero et al.

6

Table 3. Results of the partial correlation assessments between relative powers and the polysomnographic indices in the test set.

Classic bands

PSG index	RP$_{VLF}$		RP$_{LF}$		RP$_{HF}$		LF/HF	
	ρ_S	p value	ρ_S	p value	ρ_S	p value	ρ_S	p value
AHI	−0.031	0.391	**0.150**	**<0.01**	−0.075	0.040	0.118	0.001[a]
OAHI	−0.073	0.043	0.088	0.015	−0.012	0.737	0.046	0.207
OAI	−0.035	0.333	0.067	0.066	−0.031	0.392	0.052	0.154
ODI	0.039	0.289	**0.194**	**≪0.01**	**−0.161**	**≪0.01**	**0.195**	**≪0.01**
#Awakenings	**0.133**	**<0.01**	0.036	0.324	−0.115	0.014	0.086	0.018
WASO	0.071	0.049	0.112	0.002[a]	**−0.146**	**<0.01**	**0.145**	**<0.01**
%N1	0.003	0.930	0.063	0.084	−0.040	0.266	0.058	0.111
%N2	−0.085	0.019	−0.076	0.038	0.098	0.007[a]	−0.112	0.002[a]
%N3	0.068	0.060	0.074	0.043	−0.089	0.014	0.101	0.005[a]
%REM	0.041	0.262	−0.083	0.022	0.030	0.404	−0.047	0.197
TAI	0.031	0.389	**0.128**	**<0.01**	−0.098	0.007[a]	**0.126**	**<0.01**

Bands of interest

PSG index	RP$_{BW1}$		RP$_{BW2}$		RP$_{ABW1}$		RP$_{ABW2}$		RP$_{ABW3}$	
	ρ_S	p value	ρ_S	p value	ρ_S	p value	ρ_S	p value	ρ_S	p value
AHI	**−0.132**	**<0.01**	**0.233**	**≪0.01**	−0.010	0.786	−0.049	0.179	−0.101	0.005[a]
OAHI	**−0.157**	**<0.01**	**0.164**	**≪0.01**	−0.002	0.962	−0.021	0.555	−0.033	0.368
OAI	−0.096	0.008[a]	**0.149**	**<0.01**	−0.010	0.774	−0.031	0.395	−0.049	0.180
ODI	−0.033	0.358	**0.220**	**≪0.01**	−0.009	0.809	−0.100	0.006[a]	**−0.192**	**≪0.01**
#Awakenings	**0.174**	**≪0.01**	0.069	0.059	−0.036	0.329	−0.055	0.134	−0.096	0.008[a]
WASO	**0.186**	**≪0.01**	0.054	0.141	0.024	0.514	−0.046	0.210	**−0.195**	**≪0.01**
%N1	0.001	0.969	0.087	0.017	0.020	0.584	−0.005	0.887	−0.063	0.083
%N2	−0.073	0.045	−0.092	0.011	0.009	0.798	0.071	0.050	0.083	0.023
%N3	0.058	0.111	0.052	0.155	−0.028	0.443	−0.092	0.011	−0.066	0.069
%REM	0.048	0.187	−0.049	0.175	−0.004	0.913	0.019	0.594	0.041	0.262
TAI	−0.059	0.105	**0.220**	**≪0.01**	−0.025	0.492	−0.043	0.237	**−0.123**	**<0.01**

PSG polysomnographic, *RP* relative power, *VLF* very low frequency, *LF* low frequency, *HF* high frequency, *AHI* apnea–hypopnea index, *OAHI* obstructive AHI, *OAI* obstructive apnea index, *ODI* oxygen desaturation index, *WASO* wake after sleep onset, *%N1* time spent in N1 stage, *%N2* time spent in N2 stage, *%N3* time spent in N3 stage, *%REM* time spent in REM stage, *TAI* total arousals index.
[a]Non-significant after Bonferroni correction.
Values where statistically significant correlations were obtained (p value < 0.01 after Bonferroni correction) appears in bold.

polysomnographic indices considered. Despite the generally low |ρ_S| values reached, some statistically significant correlations emerged in the other bands. RP$_{BW1}$ showed positive ρ_S with macro sleep disruption-related variables (#Awakenings and WASO), while RP$_{VLF}$ showed association with #Awakenings in a lower degree than RP$_{BW1}$. RP$_{BW2}$ reached the highest absolute correlations with all the SAHS-related indices, as well as with TAI. RP$_{ABW3}$ was the only adaptive band that reached statistically significant correlations, showing negative ρ_S with ODI, WASO, and TAI. Similar to RP$_{ABW3}$, RP$_{HF}$ presented significant negative correlations with ODI and WASO but showed lower values of |ρ_S|. Indices related with sleep stages did not show any statistically significant correlations with the RPs evaluated.

Diagnostic ability assessments
Table 4 shows the results achieved by each individual RP as well as the two LDA models. The individual results showed that the highest AUC was always obtained with RP$_{BW2}$ in the three SAHS severity thresholds considered, together with the highest accuracies and specificities in 5 and 10 e/h subgroups. The only classic band that improved any result of the bands of interest was RP$_{VLF}$ (sensitivity in 1 e/h). It is noteworthy that the diagnostic performance obtained in HF was always outperformed by at least

one of the three adaptive bands of interest, except for specificity in the lowest threshold.

Finally, when LDA models were examined, the highest diagnostic performance was generally obtained with the models formed by RPs in our five bands of interest. Only specificity in 1 e/h threshold was higher with classic band model, but sensitivity/specificity pair was strongly unbalanced.

DISCUSSION
In this study, new HRV spectral bands of interest were identified and evaluated to gain insight into cardiovascular dynamics in the presence of pediatric SAHS. These bands were significantly correlated with respiratory events, as well as with micro and macro sleep disruptions. Our newly identified bands also showed a higher diagnostic yield than the widely analyzed classical spectral bands, suggesting that new spectral bands are more specific when HRV is analyzed in the pediatric SAHS context.

Physiological interpretation and usefulness of the new spectral bands of interest
BW1 (0.001–0.005 Hz) is a narrower band within VLF.[26] The physiological meaning of VLF band is under discussion,[11] and

Heart rate variability spectrum characteristics in children with sleep…
A Martín-Montero et al.

7

previous studies analyzing this band did not find differences across the pediatric SAHS severity groups.[22,23] In this study, RP$_{VLF}$ was the only parameter that did not show significant differences in any of the sets evaluated. However, RP$_{BW1}$ differed between groups in both the training and test sets, as well as showed statistically significant ρ_S with the number of awakenings and WASO in the test set. These findings suggest that, contrary to the whole VLF band, both the occurrence of the awakenings and the time spend awake is embedded in BW1. As one of the SAHS consequences is sleep fragmentation, this observation may drive the improvement in the individual diagnostic ability of RP$_{BW1}$ compared to RP$_{VLF}$ in terms of AUC.

BW2 (0.028–0.074 Hz) showed the strongest correlations with all SAHS respiratory indices (AHI, OAHI, OAI, and ODI) and TAI, the latter being composed of many respiratory-related arousals induced by the disease.[48] Furthermore, BW2 reached the highest individual diagnostic performance, clearly improving the accuracy and AUC of the remaining new and classic bands in the 5 and 10 e/h thresholds. BW2 range (0.028–0.074 Hz) comprises part of VLF and LF, which agrees with previous results reported for adults.[10] Moreover, when analyzing overnight airflow in adults, prior studies found a similar band of interest (≈0.025–0.050 Hz).[49,50] These similarities in cardiac and breathing signals may be explained by the increment in the cardio-respiratory coordination found when SAHS is present.[28] Similarly, the slight differences in the bandwidth may be explained by lower duration of cardiac events vs. respiratory events, as well as by the different annotation rules for apneic events in children and adults.[38] Such rules will score a pediatric apneic event lasting at least 2 respiratory cycles, usually corresponding to 6 s. Thus the BW2 frequency range, which reflects periodicities between 13 and 35 s, is also consistent with these annotations, while suggesting a duration for cardiac-related events. According to the above-mentioned considerations, there are robust indications that the typical SAHS-related bradycardia/tachycardia patterns are reflected in BW2, underlining the potential usefulness of this HRV band in the pediatric SAHS context.

As reflected in Fig. 2, the main differences between SAHS severity groups in the adaptive respiratory band coincide with ABW3 (samples 34–55), with averaged PSD values decreasing as SAHS worsens, and RP$_{ABW3}$ showing statistically significant differences in the training set. Moreover, ABW3 also showed statistically significant negative correlations with ODI, WASO, and TAI, which were higher than the corresponding for RP$_{HF}$. Thus the higher the power in ABW3, the lower the values will be found for oxyhemoglobin desaturations, awake time, and arousals. This finding may be indicative that normal sleep respiration activity decreases as awakening or micro awakening periods arise, which are often driven by inadequate gas exchange and, eventually, blood oxygen deficits.[1,38] This would explain the increased AUC showed by ABW3 in the three AHI thresholds compared to HF and further support the adaptive analysis rather than the fixed HF band.

ABW1 and ABW2 achieved similar diagnostic performance to HF, except in the higher severity threshold, where the diagnostic ability was markedly lower. Moreover, these two bands of interest did not show any significant correlation with the PSG indices. To investigate whether they are really useful, a final analysis was conducted. The diagnostic ability of the LDA models formed by RPs of the bands of interest with and without considering ABW1 and ABW2 is shown in Table 5. It can be appreciated that there was a slight decrease in AUC for 1 and 5 e/h thresholds when both

Table 4. Diagnostic performance in the test set for each relative power in each frequency band, as well as for both linear discriminant analysis models in terms of sensitivity (Se %), specificity (Sp %), accuracy (Acc %), and AUC.

Feature/model	AHI threshold = 1 e/h				AHI threshold = 5 e/h				AHI threshold = 10 e/h			
	Se	Sp	Acc	AUC	Se	Sp	Acc	AUC	Se	Sp	Acc	AUC
RP$_{VLF}$	68.9	31.6	56.3	0.518	33.0	65.0	60.2	0.456	40.6	64.2	62.1	0.495
RP$_{LF}$	43.5	62.9	50.1	0.557	52.7	58.4	57.6	0.590	59.4	58.4	58.5	0.666
RP$_{HF}$	35.5	71.9	47.8	0.523	39.3	68.1	63.8	0.540	43.5	76.7	73.7	0.605
LF/HF	37.7	70.3	48.7	0.540	45.5	66.8	63.7	0.567	49.3	70.8	68.8	0.643
RP$_{BW1}$	66.3	45.3	**59.2**	0.559	65.2	54.0	55.6	0.621	69.6	52.3	53.9	0.624
RP$_{BW2}$	32.7	78.1	48.1	0.591	45.5	82.0	**76.6**	0.670	58.0	78.2	76.4	0.751
RP$_{ABW1}$	52.7	49.2	51.5	0.516	41.1	59.4	56.7	0.504	55.1	39.0	40.4	0.489
RP$_{ABW2}$	49.1	55.1	51.1	0.526	36.6	69.8	64.9	0.524	44.9	47.8	47.6	0.451
RP$_{ABW3}$	45.5	56.6	49.3	0.532	44.6	64.0	61.2	0.571	49.3	64.0	62.6	0.628
LDA classic bands	25.7	81.3	44.5	0.559	46.4	72.2	68.4	0.633	50.7	75.3	73.1	0.685
LDA bands of interest	42.5	72.3	52.6	**0.592**	50.0	80.9	76.4	**0.688**	63.8	84.7	**82.8**	**0.796**

RP relative power, *VLF* very low frequency, *LF* low frequency, *HF* high frequency, *LDA* linear discriminant analysis, *AHI* apnea–hypopnea index.
The highest accuracy and AUC for each AHI threshold appears in bold.

Table 5. Diagnostic performance in the test set for both linear discriminant analysis models formed by bands of interest with and without RP$_{ABW1}$ and RP$_{ABW2}$ in terms of sensitivity (Se %), specificity (Sp %), accuracy (Acc %), and AUC.

LDA model	AHI threshold = 1 e/h				AHI threshold = 5 e/h				AHI threshold = 10 e/h			
	Se	Sp	Acc	AUC	Se	Sp	Acc	AUC	Se	Sp	Acc	AUC
With both bands	42.5	72.3	52.6	0.592	50.0	80.9	76.4	0.688	63.8	84.7	82.8	0.796
Without both bands	37.7	80.1	52.0	0.597	48.2	80.8	76.0	0.696	62.8	84.3	82.3	0.774

RP relative power, *AHI* apnea–hypopnea index.

8

bands were included, with similar accuracies, suggesting that these bands show no evidence of diagnostic utility. It also implies that only a frequency range of ≈0.04 Hz around the adaptive respiratory peak, which corresponds to the width of ABW3, would be enough to analyze HF in SAHS cases.

Comparison with previous work
To the best of our knowledge, this is the first work searching for specific HRV spectral bands of interest in the pediatric SAHS context. Previous studies in the frequency domain only analyzed the HRV classic frequency bands.[14–25]

The common finding among previous studies pointed to increased LF activity[14,21] and LF/HF ratio,[14,17,20] as well as decreased HF power[16,17,19] as SAHS worsens. Adenotonsillectomy, the common treatment for SAHS in children, reversed these trends.[18] This agrees with the results shown in Table 2. It seems that intermittent hypoxia and episodic arousals, which are present in children with SAHS and accompanied by increases in sympathetic outflow (reflected in the increased RP_{LF}) underlie the autonomic changes that persist even beyond sleep period. The effect of SAHS in the ANS was analyzed in previous studies.[51,52] Somers et al. showed that, in young healthy adults, intermittent hypoxia during sleep derived in heightened sympathetic activation, even when the stimulus was removed. In the same way, subtle changes in autonomic reactivity are detectable during arousals in healthy children as well as in children with SAHS during wakefulness.[53,54] All these evidences along with the results shown in Table 2 supports previous findings that pediatric SAHS leads to enhanced sympathetic activity, as well as decreased parasympathetic activation, resulting in impaired cardiac autonomic modulation. The absence of differences in RP_{VLF} is also in accordance with previous studies analyzing this band.[22,23]

On the other hand, previous studies originating from a single research group[23–25] conducted an automated classification of pediatric subjects into SAHS or control groups. These studies involving only 21 children derived HRV parameters from declines in amplitude fluctuations of the photoplethysmographic oximetry signal. Accuracies in the range 73.3–80.0%, together with sensitivities between 62.5 and 87.5% and specificities between 71.4 and 85.7%, were reported. Despite the similar results achieved in the present study, the different criteria used to assess SAHS presence and severity makes further comparisons difficult. Similarly, only a previous study conducted automated classification while exclusively evaluating HRV signal in pediatric SAHS context.[15] However, unlike us, this study focused on classification of each apneic event rather than each subject, such that their findings and current results cannot be compared. Thus this is the first study conducting automated classification of pediatric subjects into severity SAHS groups employing HRV signals exclusively.

Limitations and outlook
Despite the potential utility of our findings, we need to mention some of the limitations of this study. First, our LDA model performance is not yet sufficient for widespread diagnostic use, being outperformed by the results derived from the study of other polysomnographic signals such as blood oxygen saturation or airflow, which have a direct acquisition.[34,41] However, we need to remark that the aim of this study was not at optimizing classification performance but rather aimed to characterize new SAHS-specific spectral bands and compare their diagnostic ability against the classic HRV bands. Thus this is a first step that justifies future explorations of more complex predictive models with the aim to further improve the diagnostic usefulness and characterization of these novel bands. Finally, despite the robust associations found for BW1, BW2, and ABW3 relative to standard PSG indices, both ABW1 and ABW2 need further investigation to clarify their significance in pediatric SAHS.

CONCLUSIONS
This is the first study whereby specific HRV spectral bands of interest in pediatric SAHS have been identified and characterized. We have defined three new spectral bands that show significant associations with SAHS disease severity: BW1 (0.001–0.005 Hz), related to macro sleep disruptions; BW2 (0.028–0.074 Hz), related to the duration of apneic events; and ABW3, an adaptive band within the respiratory range, related to oxyhemoglobin desaturations and sleep disruption. Higher individual and collective diagnostic ability were achieved by the RPs of the new bands compared with the classical RPs for SAHS severity thresholds of 1, 5, and 10 e/h. An LDA model that incorporated five RPs from the new spectral bands achieved the highest diagnostic performance (82.8% Acc, 0.796 AUC for 10 e/h threshold). Hence, our results suggest that the new HRV bands provide more specific information on pediatric SAHS and that such novel information could be used to develop advanced automated SAHS detection methodologies. Thus future studies incorporating these novel spectral bands should be pursued to further establish their clinical significance and clinical applications.

AUTHOR CONTRIBUTIONS
A.M.-M. analyzed and interpreted data, drafted the manuscript, and approved the final version. G.C.G.T. designed the study, analyzed and interpreted data, revised the manuscript, and approved the final version. L.K.-G. acquired data, recruited and diagnosed patients, revised the manuscript, and approved the final version. J.J.-G. analyzed and interpreted data, revised the manuscript, and approved the final version. D.Á. interpreted data, revised the manuscript, and approved the final version. F.d.C. obtained funding, revised the manuscript, and approved the final version. D.G. designed the study, acquired data, recruited and diagnosed patients, revised the manuscript, and approved the final version. R.H. designed the study, obtained funding, revised the manuscript and approved the final version.

ADDITIONAL INFORMATION
Competing interests: The authors declare no competing interests.

Patient consent: The informed consent to be considered in the research was obtained from all participants and the study protocol was approved by the Ethics Committee of the Comer Children's Hospital of the University of Chicago (reference numbers #11-0268-AM017, #09-115-B-AM031, and #IRB14-1241).

Publisher's note Springer Nature remains neutral with regard to jurisdictional claims in published maps and institutional affiliations.

REFERENCES
1. American Thoracic Society. Standards and indications for cardiopulmonary sleep studies in children. *Am. J. Respir. Crit. Care Med.* **153**, 866–878 (1996).
2. Marcus, C. L. et al. Diagnosis and management of childhood obstructive sleep apnea syndrome. *Pediatrics* **130**, e714–e755 (2012).
3. Wise, M. S. et al. Executive summary of respiratory indications for polysomnography in children: an evidence-based review. *Sleep* **34**, 389–398 (2011).

Heart rate variability spectrum characteristics in children with sleep…
A Martín-Montero et al.

9

4. Iber, C., Ancoli-Israel, S., Chesson, A. L. & Quan, S. F. *The AASM Manual for the Scoring of Sleep and Associated Events: Rules, Terminology and Technical Specifi-cations* (AASM, 2007).

5. Zamarrón, C., Romero, P. V., Gude, F., Amaro, A. & Rodriguez, J. R. Screening of obstructive sleep apnoea: heart rate spectral analysis of nocturnal pulse oximetric recording. *Respir. Med.* **95**, 759–765 (2001).

6. Esnaola, S., Durán, J., Infante-Rivard, C., Rubio, R. & Fernández, A. Diagnostic accuracy of a portable recording device (MESAM IV) in suspected obstructive sleep apnoea. *Eur. Respir. J.* **9**, 2597–2605 (1996).

7. Acharya, U. R., Joseph, K. P., Kannathal, N., Lim, C. M. & Suri, J. S. Heart rate variability: a review. *Med. Biol. Eng. Comput.* **44**, 1031–1051 (2006).

8. Guilleminault, C., Winkle, R., Connolly, S., Melvin, K. & Tilkian, A. Cyclical variation of the heart rate in sleep apnoea syndrome. *Lancet* **323**, 126–131 (1984).

9. Gozal, D., Hakim, F. & Kheirandish-Gozal, L. Chemoreceptors, baroreceptors and autonomic deregulation in children with obstructive sleep apnea. *Respir. Physiol. Neurobiol.* **185**, 177–185 (2013).

10. Gutiérrez-Tobal, G. C., Álvarez, D., Gomez-Pilar, J., Del Campo, F. & Hornero, R. Assessment of time and frequency domain entropies to detect sleep apnoea in heart rate variability recordings from men and women. *Entropy* **17**, 123–141 (2015).

11. Penzel, T., Kantelhardt, J. W., Grote, L., Peter, J. H. & Bunde, A. Comparison of detrended fluctuation analysis and spectral analysis of heart rate variability in sleep and sleep apnea. *IEEE Trans. Biomed. Eng.* **50**, 1143–1151 (2003).

12. Al-Angari, H. M. & Sahakian, A. V. Use of sample entropy approach to study heart rate variability in obstructive sleep apnea syndrome. *IEEE Trans. Biomed. Eng.* **54**, 1900–1904 (2007).

13. Gong, X. et al. Correlation analysis between polysomnography diagnostic indices and heart rate variability parameters among patients with obstructive sleep apnea hypopnea syndrome. *PLoS ONE* **11**, 1–13 (2016).

14. Baharav, A., Kotagal, S., Rubin, B. K., Pratt, J. & Akselrod, S. Autonomic cardio-vascular control in children with obstructive sleep apnea. *Clin. Auton. Res.* **9**, 345–351 (1999).

15. Cohen, G. & de Chazal, P. Automated detection of sleep apnea in infants: a multi-modal approach. *Comput. Biol. Med.* **63**, 118–123 (2015).

16. Liao, D. et al. Sleep-disordered breathing and cardiac autonomic modulation in children. *Sleep Med.* **11**, 484–488 (2010).

17. Liao, D. et al. Sleep-disordered breathing in children is associated with impair-ment of sleep stage-specific shift of cardiac autonomic modulation. *J. Sleep Res.* **19**, 358–365 (2010).

18. Muzumdar, H. V. et al. Changes in heart rate variability after adenotonsillectomy in children with obstructive sleep apnea. *Chest* **139**, 1050–1059 (2011).

19. Walter, L. M. et al. Autonomic dysfunction in children with sleep disordered breathing. *Sleep Breath.* **17**, 605–613 (2013).

20. Van Eyck, A. et al. Sleep disordered breathing and autonomic function in over-weight and obese children and adolescents. *ERJ Open Res.* **2**, 1–8 (2016).

21. Horne, R. S. C. et al. The impact of sleep disordered breathing on cardiovascular health in overweight children. *Sleep. Med* **41**, 58–68 (2018).

22. Kwok, K. L. et al. Heart rate variability in childhood obstructive sleep apnea. *Pediatr. Pulmonol.* **46**, 205–210 (2011).

23. Gil, E. et al. Discrimination of sleep-apnea-related decreases in the amplitude fluctuations of ppg signal in children by HRV analysis. *IEEE Trans. Biomed. Eng.* **56**, 1005–1014 (2009).

24. Gil, E., Bailón, R., Vergara, J. M. & Laguna, P. PTT variability for discrimination of sleep apnea related decreases in the amplitude fluctuations of PPG signal in children. *IEEE Trans. Biomed. Eng.* **57**, 1079–1088 (2010).

25. Lázaro, J., Gil, E., Vergara, J. M. & Laguna, P. Pulse rate variability analysis for discrimination of sleep-apnea-related decreases in the amplitude fluctuations of pulse photoplethysmographic signal in children. *IEEE J. Biomed. Health Inform.* **18**, 240–246 (2014).

26. Task Force of the ESC and the NSA of Pacing and Electrophysiology. Heart rate variability. Standards of measurement, physiological interpretation, and clinical use. *Circulation* **93**, 1043–1065 (1996).

27. Michels, N. et al. Determinants and reference values of short-term heart rate variability in children. *Eur. J. Appl. Physiol.* **113**, 1477–1488 (2013).

28. Riedl, M. et al. Cardio-respiratory coordination increases during sleep apnea. *PLoS ONE* **9**, e93866 (2014).

29. Seppälä, S. et al. Normal values for heart rate variability parameters in children 6-8 years of age: The PANIC Study. *Clin. Physiol. Funct. Imaging* **34**, 290–296 (2014).

30. Goren, Y., Davrath, L. R., Pinhas, I., Toledo, E. & Akselrod, S. Individual time-dependent spectral boundaries for improved accuracy in time-frequency analysis of heart rate variability. *IEEE Trans. Biomed. Eng.* **53**, 35–42 (2006).

31. Milagro, J. et al. Noninvasive cardiorespiratory signals analysis for asthma evo-lution monitoring in preschool children. *IEEE Trans. Biomed. Eng.* **9294**, 1–1 (2019).

32. Milagro, J. et al. Nocturnal heart rate variability spectrum characterization in preschool children with asthmatic symptoms. *IEEE J. Biomed. Health Inform.* **22**, 1332–1340 (2018).

33. Fleming, S. et al. Normal ranges of heart rate and respiratory rate in children from birth to 18 years of age: a systematic review of observational studies. *Lancet* **377**, 1011–1018 (2011).

34. Vaquerizo-Villar, F. et al. Wavelet analysis of oximetry recordings to assist in the automated detection of moderate-to-severe pediatric sleep apnea-hypopnea syndrome. *PLoS ONE* **13**, 1–18 (2018).

35. Hornero, R. et al. Nocturnal oximetry-based evaluation of habitually snoring children. *Am. J. Respir. Crit. Care Med.* **196**, 1591–1598 (2017).

36. Redline, S. et al. The Childhood Adenotonsillectomy Trial (CHAT): rationale, design, and challenges of a randomized controlled trial evaluating a standard surgical procedure in a pediatric population. *Sleep* **34**, 1509–1517 (2011).

37. Marcus, C. L. et al. A randomized trial of adenotonsillectomy for childhood sleep apnea. *N. Engl. J. Med.* **368**, 2366–2376 (2013).

38. Berry, R. B. et al. Rules for scoring respiratory events in sleep: update of the 2007 AASM manual for the scoring of sleep and associated events. *J. Clin. Sleep Med.* **8**, 597–619 (2012).

39. Tan, H.-L., Gozal, D., Ramirez, H. M., Bandla, H. P. R. & Kheirandish-Gozal, L. Overnight polysomnography versus respiratory polygraphy in the diagnosis of pediatric obstructive sleep apnea. *Sleep* **37**, 255–260 (2014).

40. Barroso-García, V. et al. Irregularity and variability analysis of airflow recordings to facilitate the diagnosis of paediatric sleep apnoea-hypopnoea syndrome. *Entropy* **19**, 447 (2017).

41. Barroso-García, V. et al. Usefulness of recurrence plots from airflow recordings to aid in paediatric sleep apnoea diagnosis. *Comput. Methods Prog. Biomed.* **183**, 105083 (2020).

42. Xu, Z. et al. Cloud algorithm-driven oximetry-based diagnosis of obstructive sleep apnoea in symptomatic habitually snoring children. *Eur. Respir. J.* **53**, 1801788 (2019).

43. Benitez, D., Gaydecki, P. A., Zaidi, A. & Fitzpatrick, A. P. The use of the Hilbert transform in ECG signal analysis. *Comput. Biol. Med.* **31**, 399–406 (2001).

44. Welch, P. D. The use of fast Fourier transform for the estimation of power spectra: a method based on time averaging over short, modified periodograms. *IEEE Trans. Audio Electroacoust.* **15**, 70–73 (1967).

45. Nuwer, M. R. Quantitative EEG. I: Tecniques and problems of frequency analysis and topographic mapping. *J. Clin. Neurophysiol.* **5**, 1–43 (1988).

46. Bishop, C. M. *Patter Recognition and Machine Learning* (Springer, New York, 2006).

47. Marcos, J. V., Hornero, R., Álvarez, D., del Campo, F. & Zamarrón, C. Assess-ment of four statistical pattern recognition techniques to assist in obstructive sleep apnoea diagnosis from nocturnal oximetry. *Med. Eng. Phys.* **31**, 971–978 (2009).

48. Grigg-Damberger, M. et al. The visual scoring of sleep and arousal in infants and children. *J. Clin. Sleep. Med.* **3**, 201–240 (2007).

49. Gutiérrez-Tobal, G. C. et al. Linear and nonlinear analysis of airflow recordings to help in sleep apnoea-hypopnoea syndrome diagnosis. *Physiol. Meas.* **33**, 1261–1275 (2012).

50. Gutiérrez-Tobal, G. C., Álvarez, D., Marcos, J. V., Del Campo, F. & Hornero, R. Pattern recognition in airflow recordings to assist in the sleep apnoea-hypopnoea syndrome diagnosis. *Med. Biol. Eng. Comput.* **51**, 1367–1380 (2013).

51. Somers, V. K., Mark, A. & Abboud, F. Sympathetic activation by hypoxia and hypercapnia–implications for sleep apnea. *Clin. Exp. Hypertens.* **10**, 413–422 (1998).

52. Narkiewicz, K. & Somers, V. K. The sympathetic nervous system and obstructive sleep apnea: Implications for hypertension. *J. Hypertens.* **15**, 1613–1619 (1997).

53. O'Brien, L. M. & Gozal, D. Autonomic dysfunction in children with sleep-disordered breathing. *Sleep* **28**, 747–752 (2005).

54. O'Brien, L. M. & Gozal, D. Potential usefulness of noninvasive autonomic mon-itoring in recognition of arousals in normal healthy children. *J. Clin. Sleep. Med.* **3**, 41–47 (2007).